

Investigation of the sensing mechanism in cobalt doped ZnO matrix based on structural, morphology, optical and electrical studies

A. ZIA^{ab*}, S. AHMED^c, N. A. SHAH^d

^aGovernment Postgraduate College Asghar Mall, Rawalpindi, Pakistan

^bCenter for Emerging Sciences, Engineering & Technology (CESET), Islamabad, Pakistan

^cAdvanced Electronics Laboratories, International Islamic University, Islamabad, Pakistan

^dCOMSATS, Institute of Information Technology (CIIT), Islamabad, Pakistan

The effective role of successive cobalt doping with co-precipitation route in ZnO matrix has been explored to study the presence of sensing response on the basis of its structural, morphological, optical and electrical characterization. X-ray diffraction (XRD) analysis confirms the incorporation of Cobalt in the ZnO matrix quite effectively. The increased bond length Zn-O in (002) plane on cobalt addition corresponds to an increase in the volume of unit cell. Scanning Electron Microscopy (SEM) provides further insight to the morphological features of the cobalt doped ZnO nanoparticles having spherical shape of increased dimensions. Fourier Transform infrared (FTIR) Spectroscopy reveals the incorporation of cobalt along with the presence of functional chemical bonding in the ZnO matrix. The observed peaks ranging from 1200-1700 cm^{-1} correspond to Zn-OH bonding mode. The red shifted optical energy band gap is used to estimate the refractive index and found to be of small value in pure ZnO than the cobalt doped samples. An in-depth electrical characterization with two and four probe techniques provides an increase in the sheet resistance and resistivity with cobalt addition. Secondly, the reduction in photo electric resistance proves the existence of sensing mechanism in ZnO matrix. The variation in Hall mobility and voltage confirms the extrinsic semiconductor character of ZnO matrix for different cobalt contents. The effect of cobalt on these distinct parameters can be exploited for the bio-sensing and optoelectronic device engineering due to its biocompatibility, electron mobility and high surface to volume ratio.

(Received September 13, 2016; accepted April 5, 2018)

Keywords: ZnO, Nano structure, Refractive index, Bond length, Resistivity, Biosensors

1. Introduction

The critical role of dilute magnetic semiconductor oxides (DMSO) at nanoscale has attracted many researchers to study their unusual physical properties and potential applications in the novel device fabrication [1]. Intensive research efforts has been carried out to explore the effect of magnetic dopants in the nonmagnetic semiconductor host specially TiO_2 and ZnO [2]. Over the past decades, nanomaterial engineering has been carried out due to their high sensitivity, smaller size, quantum confinement and high aspect ratio [3]. The physical properties of the nanomaterial changes drastically due to change in the band gap, which depends upon the impurity concentration. This makes the material suitable for future smart bio-sensing devices.

ZnO is considered as a renowned inorganic metal oxide semiconductor due to its n-type conductivity, high excitonic energy (60 meV), wide optical energy band gap (3.37eV) and high optical gain (320 cm^{-1}) at room temperature [4-10]. Such promising features of ZnO advances it for next generation of short wavelength optoelectronic device applications like light emitting diodes, solar cells, UV sensors, varistors, and laser diodes [11-17]. ZnO is also considered as an effective candidate

for spintronics devices due to existence of ferromagnetic character at room temperature when doped with small amount of 3-d transition metal ions such as Mn^{+2} , Fe^{+3} , V^{+3} , Ni^{+2} and Co^{+2} [18-21].

There are numerous techniques to tailor the structural, optical and electrical properties of metal oxides based nanostructures. The most effective is the implantation of dopant in to the host matrix. The dopant element (either cationic or anionic), stabilizes the surface of the host ZnO and can alter the grain size too. In hexagonal polar symmetry, the tetrahedral coordinated O^{2-} with Zn^{2+} plays an important role to exploit its physical, chemical and surface properties to determine the immobilization technique for the biosensors sensitivity. Moreover, the high aspect ratio, biocompatibility and good electron transfer rate of the ZnO nanostructure can improve the enzyme loading rate, drug delivery systems and electrochemical nature of biomolecules [22-23]. Secondly, the optical sensing and antibacterial activity in pure ZnO nanoparticles is also strongly related with the surface defects and the availability of oxygen vacancies on large surface area of the nanoparticles. The vacancies concentration can be increased by the replacement of Zn ions in the host matrix. Many research groups explain the effect of different doping concentrations of transition

metals on the physical properties of ZnO nanostructures to investigate the magnetic, photoconductive and antibacterial response [24-28].

The composition, grain size, purity and morphology of the samples are strongly dependent on the synthesis techniques. Many processes, such as Sol gel; electrodeposition, hydrothermal, co-precipitation, Physical Vapour Deposition (PVD), Chemical Vapour Deposition (CVD) and gas condensation etc. are employed for the fabrication of ZnO nanostructures of different shapes. ZnO nanostructures have also been developed by using co-precipitation method owing many advantages like low cost, easier composition control to obtain c-axis orientation and easy route of synthesis.

In this present study, we are exploring the different sensing mechanisms of un-doped and cobalt doped ZnO nanostructures on the basis of its structural, morphological, compositional, optical and electrical characteristics. The influence of cobalt addition in ZnO matrix can be employed to investigate the change in structural, optical and electrical parameters such as bond length Zn-O along the c-direction for the plane (002), atomic packing factor, u-positional internal parameter, dislocation density, lattice strain, refractive index, electrical resistance and various Hall-effect parameters. This detailed analysis is important in order to exploit the fabricated structure for biosensors, optoelectronic device engineering and number of other technological applications.

2. Experimental

The precursors in desired quantity (ZnCl_2 , CoCl_2 and NaOH) were mixed with de ionized water at room temperature to prepare the 1.0 M, 0.1 M and 2.0 M solution. 20 ml ZnCl_2 was then added drop-wise to 17 ml NaOH along with 43 ml of deionized water and CoCl_2 solution (2, 6, 10, 16 and 20 ml) to make five samples of desired cobalt concentration. Samples were subsequently annealed at 600°C for two hours after filtration and drying. Palletisation was performed under pressure of about 1MPa followed by another run of annealing at 1000°C for three hours. Detailed experimental process is also deliberated in some of our earlier published work on ZnO nanostructures [30].

3. Structure and Morphology

The structural features have been studied through XRD with PAN analytical spectrometer model X'PERT PRO. Effect of cobalt doping on the structural parameters like lattice parameters, d-spacing and crystallite size have been reported earlier [29-30]. All the peaks were indexed with respect to hexagonal wurtzite structure using corresponding card 01-073-8765 (space group-P63mc) and found to be shifted towards decreasing angle on cobalt addition as presented in Fig. 1. The maximum peak shift of 0.07° in plane (101) has been observed. Average

crystallite size had been estimated by Scherer's equation [10] and found to be increasing on cobalt addition ranging from 97 nm-169 nm due to left peak shifting as reported earlier in our work [19].

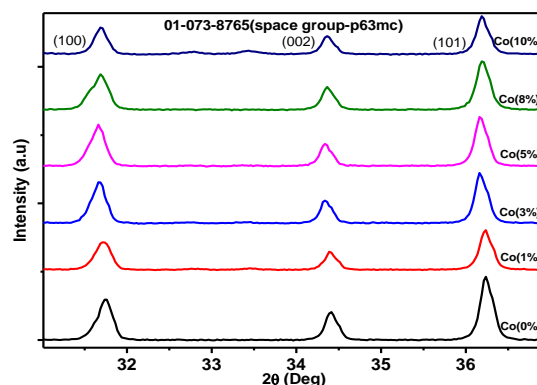


Fig.1. XRD pattern for most intensive Peaks of different cobalt doping levels

In present study, we are exploring the structural data to estimate atomic packing factor (c/a), dislocation density [33], lattice strain [33] and internal positional parameter (u) to study the influence of cobalt doping on the physical properties of the host matrix. The internal positional parameter (u) is calculated using relation (1). Both APF and internal positional parameter is found to be constant for all cobalt concentrations as shown in Figure 2(a). The bond length Zn-O (L) along the c-direction is measured using relation (2) and found to be increasing with cobalt addition [3]:

$$u = \frac{1}{3} \left(\frac{a^2}{c^2} \right) + \frac{1}{4} \quad (1)$$

$$L = \sqrt{\frac{a^2}{3} + \left(\frac{1}{2} - u \right)^2 c^2} \quad (2)$$

This increase in bond length confirms the tetrahedral coordination of cobalt in the ZnO matrix. Secondly, increase in bond length is thought to be responsible for the increase in the volume of the unit cell with cobalt addition as presented in Figure 2(b). The variation in Full Width at Half Maximum (FWHM) and bond length (L) with the incorporation of cobalt content has an inverse effect as presented in Figure 2(c), which is in accordance with the variation in crystallite size according to the Scherer's equation. A uniform disparity has also been observed between lattice strain and dislocation density for all cobalt concentrations as exhibited in Fig. 2(d). Such type of disparities in structural parameters on cobalt addition may be caused due to presence of oxygen vacancies the in ZnO matrix has been reported by many research groups [2-3], [25-28]. These estimated parameters are depicted in Table 1. The observed anomalies in microstructural parameters like atomic packing factor (APF), dislocation density and lattice strain has significant effect on the physical properties of the ZnO matrix for the development of novel and smart devices.

Table 1. Measured values of FWHM, atomic packing factor, u-parameter, bond length, dislocation density and lattice strain in Co-doped ZnO nanostructures

Co Doping%	FWHM	Atomic Packing factor c/a	Positional parameter u	Bond length L(A ^o)	Dislocation density(m ⁻²) 10 ¹⁴	Strain(e) 10 ⁻⁴
0	0.1492	1.633	0.375	7.060	1.232	3.602
1	0.1274	1.633	0.375	7.097	0.806	2.702
3	0.1350	1.633	0.375	7.074	0.977	3.038
5	0.1533	1.633	0.375	7.074	1.507	3.782
8	0.1486	1.633	0.375	7.069	1.194	3.522
10	0.1420	1.633	0.375	7.069	1.053	3.254

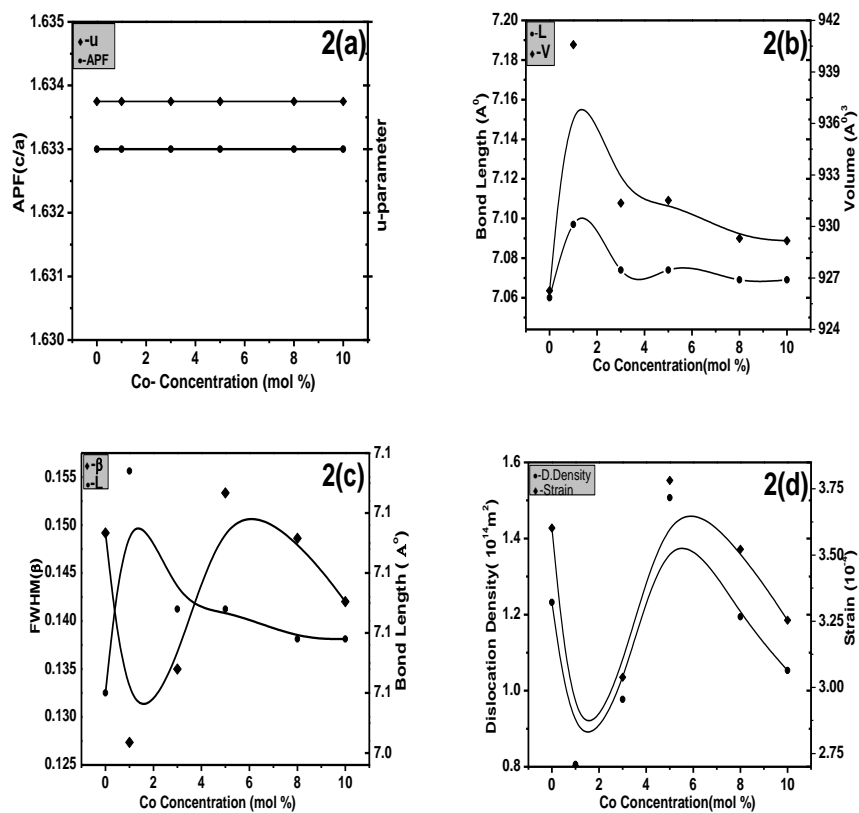


Fig. 2(a) APF (c/a) and u-parameter, (b) Bond length and volume of unit cell, (c) FWHM and bond length and (d) Dislocation density and lattice strain with cobalt contents

In order to study the key role of cobalt content in ZnO matrix, morphological and compositional analysis was employed with SU-1500 Scanning Electron Microscope (SEM) at 10 KV with micro marker of 30 μ m for the pellets. SEM micrographs have been presented in Fig. 3.

These recorded results prove the formation of spherically shaped agglomerated particles of increasing size with the cobalt addition in ZnO matrix. The average estimated size ranges from 1.2 μ m -2.5 μ m. The slightly large dimensions are due to possible agglomeration of the particles under high pressure during the palletizing process and different annealing time cycles as compared to the conventional powdered form used for XRD [36].

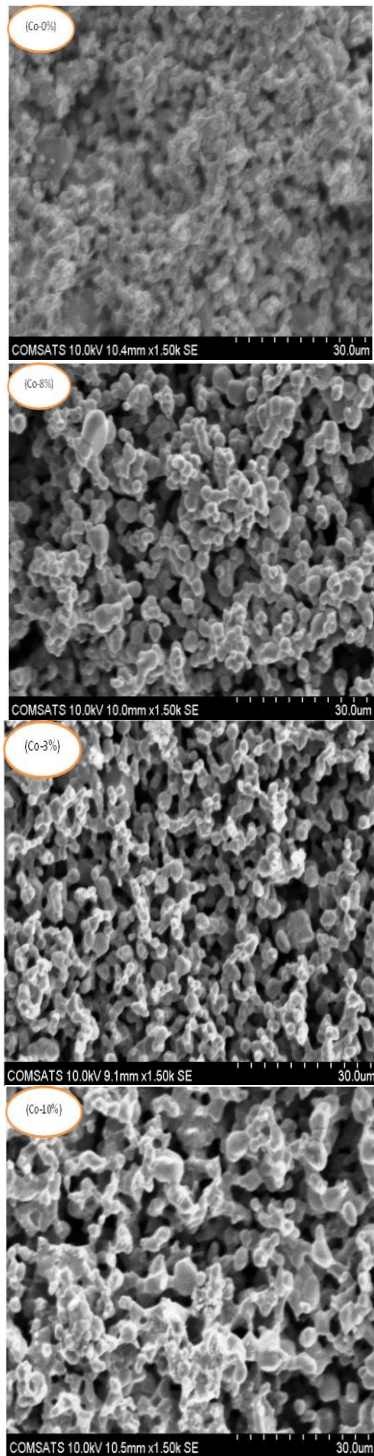


Fig. 3. SEM- micrographs for various Co-content in ZnO nanostructures (0%, 3%, 8% and 10%)

4. Fourier Transform Infra-Red (FTIR) Spectroscopy

The characteristics of optoelectronic and bio-sensing devices are strongly dependent on the impurity density incorporated in ZnO lattice. To analyse the presence of very small contents of impurity and chemical bonding in the host matrix along with the radiative behaviour of the

ZnO nanostructures; FTIR has been considered as a powerful and supportive technique to compare the results obtained from XRD, SEM and EDS. FTIR spectroscopy was performed using KBr pellet methodology with wavenumbers ranging from 4000 to 400 cm^{-1} as presented in Fig. 4. No cobalt peak has been observed in FTIR spectra, which confirms that Zn has been replaced with Cobalt in the ZnO matrix. This result is in accordance with the XRD analysis presented above.

The main absorbance peaks observed in all the samples ranging from 1200-1700 cm^{-1} correspond to Zn-OH bending mode and also to a weak band at 2960 cm^{-1} assigned to the

O-H stretching modes have been also explained by Diaja *et al* [38]. Similarly, few absorption peaks in the range 400-500 cm^{-1} may be attributed to the stretching modes of Zn-O at octahedral sites, which confirms the formation of wurtzite structure. The development of different chemical bonding mechanism may increase the sensing characteristics of the ZnO matrix on the possible interaction with biomolecules like antibody, protein and enzymes etc. Such sort of behaviour has also been reported by some other research groups [35, 39].

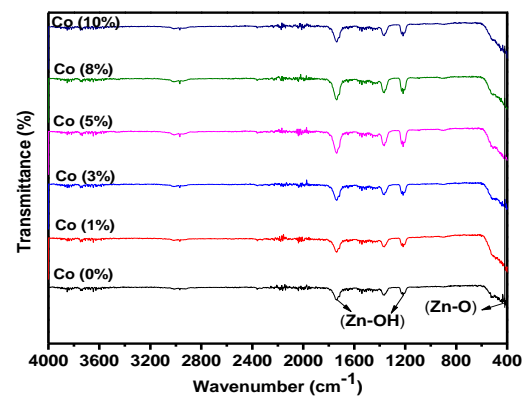


Fig. 4. FTIR spectra for all cobalt contents in ZnO matrix.

5. Refractive index

The study of refractive index plays an important role for the novel optoelectronic and bio-photonics device engineering [1, 24]. The same was studied by λ -950 (Perkin-Elmer spectrophotometer) with integrating sphere attachment and spectral on-reflectance standards. The diffused reflectance data was recorded with in the wave length ranging from 250-800 nm and transformed to square of the Kubelka- Munk to calculate the optical energy band gap and was found to be red shifted within the range of 3.17 - 2.77 eV. In order to investigate the refractive index from energy band gap, Moss relation is used as expressed in relation 3 below [24]:

$$n = 4 \sqrt{\frac{k}{E_g}} \quad (3)$$

Where $k = 108$ eV (constant value for semiconductor materials) is the threshold energy corresponding to the absorption edge and E_g is the respective optical energy

band gap. The estimated values of refractive indices for all Cobalt concentrations ranges from 2.42 to 2.49 and found to be increasing with the addition of cobalt in ZnO matrix, as summarized in Table 2. Increase in refractive index with the decrease in energy band gap is in accordance with the Moss relation. Same sort of cobalt behaviour in ZnO matrix has also been seen by Prakash and Anuragh [24]. The correlation in optical energy band gap and refractive index with the increasing Cobalt content in ZnO nanostructures is expressed in Fig. 5.

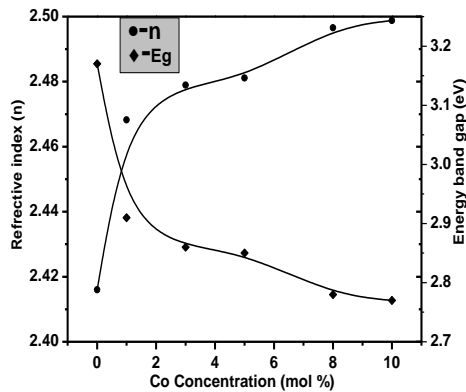


Fig. 5. Refractive index and optical energy gap with different cobalt doping levels.

6. Electrical Analysis

6.1. Two point probing Technique

Electrical behaviour of nanomaterial is strongly dependent on the intrinsic defects generated during the synthesis and the dopant concentration. Electrical resistance of all the pellets was studied earlier using Keithly SCS 420 system with two probe technique. Measurements were done at room temperature and recorded by the variation of current with respect to applied potential of $\pm 10V$ as pictured in Fig. 6. As the presence of cobalt at tetrahedral sites in ZnO matrix can enhance the volume of the unit cell [33], which may be responsible for the increase in resistance and resistivity on cobalt addition in ZnO matrix.

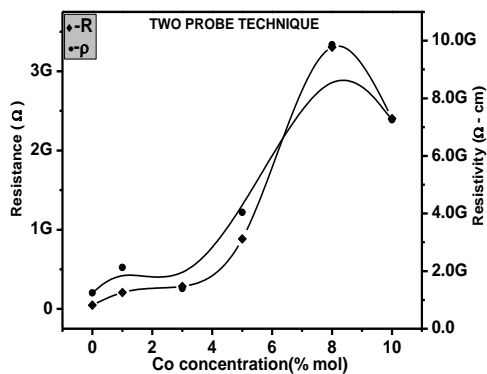


Fig. 6. Variation in resistance and resistivity with cobalt addition in ZnO matrix measured by Two-point probe technique

6.2. Hall parameters by four point probing Technique

Measurement precision has significant role to estimate the values of Hall parameters like sheet resistance, resistivity, Hall voltage and mobility etc. for exploitation in the semiconductor nanoscale device manufacturing. The Four Probe Technique (FPT) is thus used to measure the pronounced parameters by using SWIN Hall Effect system 8800, under applied current of 1 mA and applied magnetic field of 5300 G. The measured values of hall parameters are tabulated in Table 2. Conductivity of n-type semiconductors like ZnO relates with the movement of electrons in conduction band and strongly depends on the defects produced by the oxygen vacancies at room temperature. Similar trends have been observed in the measured values of resistivity by both the techniques as presented in Fig. 7. The Two Probe Technique predicts quite high values as compared to the Four Probe Technique. In FPT, additional applied magnetic field may influence the grain boundaries and can reduce the forbidden band gap even further. Such behavior may be responsible for the low values of resistivity. Secondly, the Hall voltage is positive for the sample with cobalt content of 1%, which provides an evidence of the presence of P-type carriers in ZnO nanostructures. In contrast, all other samples with varied Cobalt content show the n-type character. Hall mobility and voltage for all samples are presented in Figure 8. The high resistivity and low mobility in the samples suggests that cobalt may behave as deep donor in the ZnO matrix and may be responsible to reduce the intrinsic donor density [6]. Moreover, the tetrahedral coordination of oxygen with cobalt ion is weaker than Zn in the host matrix, which can increase the density of vacancies and the distortion in the crystal lattice. This is thought to be responsible for the increase in resistivity and decrease in mobility values with the cobalt addition in ZnO matrix [33]. In the highest cobalt concentration sample (10%); the decrease in the resistivity resulted in an increase in carrier mobility which may be triggered due to the presence of anti-ferromagnetic character of cobalt oxides as explained earlier in our work [19, 30].

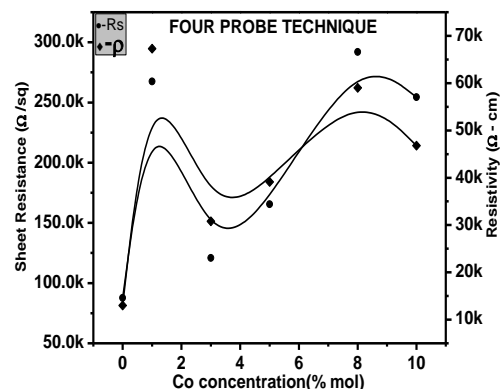


Fig. 7. Variation in Sheet resistance and resistivity with cobalt addition by FPT

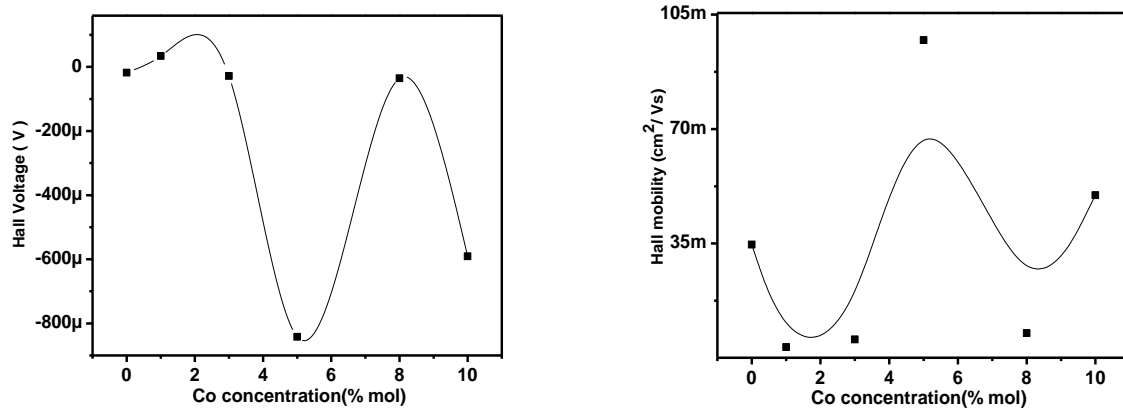


Fig. 8: Variation in Hall voltage and Hall mobility with cobalt addition in ZnO matrix

Table 2: Measured values of refractive index and Hall Parameters

Co Doping %	n	R(TPT) $\times 10^8$ (Ω)	R_s (FPT) $\times 10^5$ (Ω /Sq)	R_p (TPT) $\times 10^8$ (Ω)	ρ (TPT) $\times 10^9$ (Ω -cm)	ρ (FPT) $\times 10^4$ (Ω -cm)	V_H $\times 10^{-5}$ (V)	μ_H (cm^2/Vs)
0	2.416	2.01	0.88	0.814	0.82	1.30	-1.79	0.03463
1	2.468	5.23	2.68	3.414	1.26	6.73	3.43	0.00328
3	2.479	2.58	1.21	1.227	1.47	3.08	-2.87	0.00568
5	2.481	12.2	1.66	7.969	3.11	3.91	-84.2	0.09719
8	2.497	33.4	2.92	27.82	9.78	5.90	-3.56	0.00758
10	2.499	23.9	2.55	16.20	7.30	4.68	-59.1	0.04979

7. Approach to ZnO based sensors

In order to explore the optical sensing response in the matrix photo electric resistance (R_p) is measured by exposing the pellets with UV light. The electromagnetic energy more than optical energy band gap can generate the electron-hole pairs in the matrix to increase the conductance and decrease the resistance. This result proves the development of sensing response in ZnO matrix

that is strongly related with the surface defects. On exposing with UV light electron density in conduction band is increased due to the intrinsic defects generated by the oxygen vacancies and the atmospheric adsorption of oxygen thought to be responsible for reducing values of photo electric resistance [6-39]. The photo conductive response for all cobalt concentrations is depicted in Fig. 9.

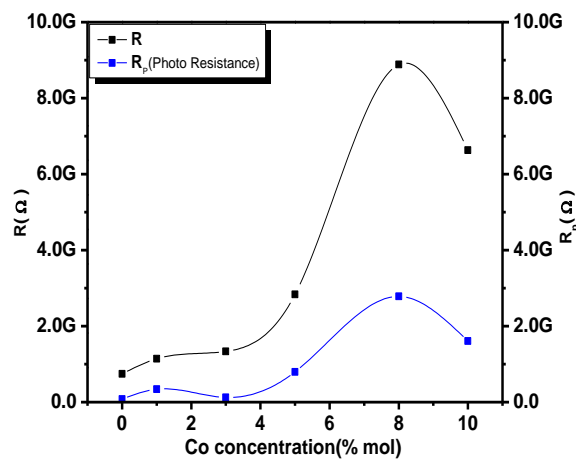


Fig. 9: Reduction in Photo electric resistance for all cobalt contents in ZnO matrix

Similarly due to biomimetic semiconductor nature, ZnO matrix has been used for the binding activity of various bio sensing molecules like enzymes, anti-gens,

proteins and DNA. A schematic ZnO biosensor is shown in Fig. 10.

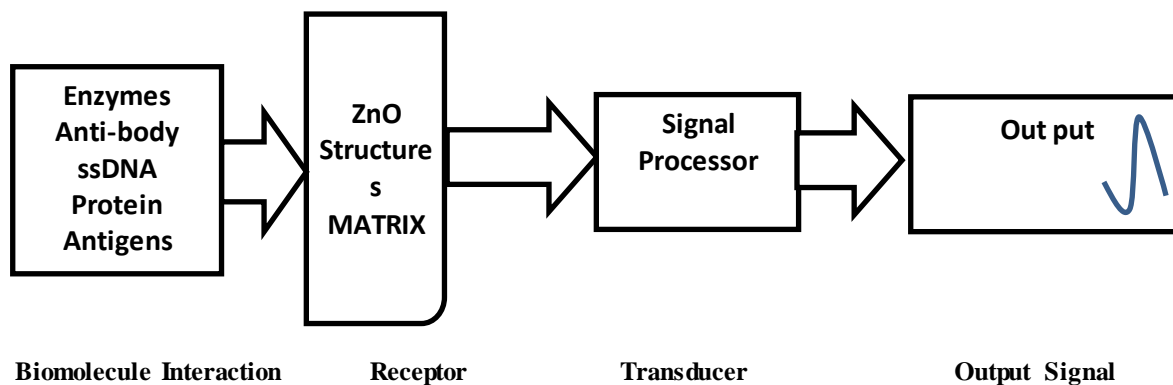


Fig. 10. A Schematic representation of ZnO biosensor

The presence of two interacting sub-lattices of Zn^{+2} and O^{-2} in ZnO matrix with Zinc ion surrounded by tetrahedral oxygen ions produced due to surface defects and linked with the study of dislocation density and lattice strain on cobalt addition is responsible for the development of antibacterial activity [22,26]. Similarly, on doping the charge concentration will change due to fewer electrons in Co as compared with Zn, which may reduce the crystal potential and increase the biological effectiveness of binding various bio sensing molecules on interaction with cobalt doped nanostructure. Thus cobalt doped ZnO matrix provides a solid support for the binding of biomolecules and its stability due to the surface morphology on the basis of immobilization and cross linking techniques. Further, the source matrix can change the resistance of the biomolecule to detect different physical and chemical changes, like temperature, composition and variation in pH value of the sensing mechanism. These changes can be purported and transduced accordingly. These variations can be detected and processed to develop an output signal pulse. Such type of bio-sensing mechanisms in cobalt doped ZnO has also been proposed by Arya *et al* [22]. The operational stability of the sensor strongly depends upon the physical and chemical properties of the matrix for the development of immobilization techniques. Due to easy surface modification, electro-catalytic activity, high electron mobility, high surface to volume ratio, high adsorption and binding with biomolecules; cobalt doped ZnO nanostructures are considered potential candidate over other material for novel device engineering of biosensors. The results presented in this work have ramifications for the design and fabrication of such devices used in optoelectronic and bio-sensing applications.

8. Conclusion

Cobalt doping effects in pure ZnO have been explored to analyze the photoconductive and antibacterial activity

and evaluate the possible sensing mechanism. It is found that the presence of oxygen vacancies can enhance the antibacterial activity in Co-ZnO nanoparticles. Further; SEM micrographs confirm the spherical shape of the particles with increasing dimensions with addition of cobalt content therein. FTIR analysis explains the presence of chemical bonding in ZnO matrix and eliminates the probability of having a cobalt phase. Increase in the refractive index is also observed on cobalt addition due to the Red shift in optical energy band gap. Electrical analysis with two- and four-point probe techniques reveal an increase in resistance, sheet resistance and resistivity, and a relative decrease in the Hall mobility with increase in the cobalt content. Decrease in photo electric resistance signifies the presence of photo conductive response of the ZnO based sensors. This study also provides a competitive edge to the Four-Probe method over the Two-probe, owing its measurement precision at nanoscales for such materials and devices. These highlighted features, both in terms of processing and careful characterization of cobalt doped ZnO nanostructure, may be exploited further to fabricate efficient, fast responsive and increasingly sensitive devices.

Innovation character

Increase in refractive index and resistance with the decrease in optical energy band gap and decrease in photo electric resistance provides an insight for the scientists to design and fabricate novel and smart optoelectronics device structures along with sensing mechanism for smart optoelectronic and biosensor engineering.

References

- [1] Yasemin Caglar, J. Alloys Compd. **560**, 181 (2013).
- [2] S. B. Ogale, Adv. Mater. **22**, 3125 (2010).

- [3] M. Mehedi et al., *Journal of Luminescence* **145**, 160 (2014).
- [4] Sha Wang, Ping Li, Hui Liu, Jibiao Li, Yu Wei, *J. Alloys Compd.* **505**, 362 (2010).
- [5] Shafique et.al. *International Nano letters* **2**(3), 1.5326-2-31 (2012).
- [6] M. L. Dinesha, H. S. Jayanna, S. Mohanty, S. Ravi. *Journal of Alloys and Compounds* **490**, 618 (2010).
- [7] M. G. Nair et al., *Materials Letters* **65**, 1797 (2011).
- [8] Amanpal Singh, D. Kumar et al., *Journal of Electrochemical Society* **158**(1) G9 (2011).
- [9] G. Murugadoss, J. Master. *Sci. Technol.* **28**(7), 587 (2012).
- [10] S. A. Ansari, Ambreen Nisar, Bushra Fatima, Wasi Khan, A. H Naqvi, *J. of Material Science and Engineering* **B177**, 428 (2012).
- [11] L. C. Chen, C. H. Tien, W. C. Liao, Y. M. Luo, *J. Lumin.* **131**, 1234 (2011).
- [12] D. C. Look, B. Claflin, *Phys. Status Solidi* **241**, 624 (2004).
- [13] Mariem Chaari et al., *J. of Materials Sciences and Applications* **2**, 765 (2011).
- [14] S. Major, K. L. Chopra, *Solar Energy Materials* **17**(5), 319 (1988).
- [15] T. K. Gupta, *J. Am. American Ceramic Society* **73**(7), 1817 (1990).
- [16] S. Anas, R. V. Mangalaraja, M. Poothayal, S. K. Shukla, S. Anantha Kumar, *Acta Materialia* **55**(17), 5792 (2007).
- [17] A. Mitra, R. K. Thareja, *J. Appl. Phys* **89**, 2025 (2001).
- [18] Lin Hsiu-Fen, Liao Shih-Chieh, Hung Sung-Wei, *J. Photoch Photobio. A* **174**, 82 (2005).
- [19] A. Zia et al., *Phys. Scr.* **89**, 105802 (2014).
- [20] C. K. Ghosh, K. K. Chattopadhyay, M. K. Mitra, *J. Appl. Phys.* **101**, 124911 (2007).
- [21] S. Guo et al., *J. of Chemical Physics Letters* **459**, 82 (2008).
- [22] S. K. Arya et al., *Analytica Chimica Acta* **737**, 1 (2012).
- [23] Z. H. Dai, G. J. Shao, J. M. Hong, J. C. Bao, J. Shen, *Biosens. Bioelectron* **24**, 1286 (2009).
- [24] Prakash Chand, Anurag Gaur, Ashavani Kumar: *IJCMNMM Engg.* **8**(12), 1288 (2014).
- [25] S. B. Rana, R. P. P. Singh, *J. of Mater Sci: Mater. Electron.* **27**, 9346 (2016).
- [26] S. B. Rana, R. P. P. Singh, Sandeep Arya, *J. of Mater Sci: Mater. Electron.* **28**, 2660 (2017).
- [27] R. P. P. Singh, I. S. Hudiara, Sudhaker Panday, S. B. Rana, *J. of Superconductivity and Novel Magnetism* **28**, 3685 (2015).
- [28] R. P. P. Singh, I. S. Hudiara, Sudhaker Panday, Pushpendra Kumar, S. B. Rana, *J. Nano-electronics and Materials* **9**, 1 (2016).
- [29] A. Zia et al. *Physica B* **473**, 42 (2015).
- [30] A. Zia et al. *Phys. Scr.* **90**, 065503 (2015).
- [31] Shiv Kumar, Subhrajit Mukherjee, Ranjan Kr. Singh, S. Chatterjee, A. K. Ghosh, *J. Appl. Phys.* **110**, 103508 (2011).
- [32] G. P. Joshi, N. S. Saxena, R. Mangal, A. Mishra, T. P. Sharma, *Mater. Sci. Indian Academy of Sciences* **26**, 387. (2003).
- [33] M. Naeem, S. K. Hasanain, A. Mumtaz, *J. Phys. Condens. Matter* **20**, 025210 (2008).
- [34] Y. Q. Chang et al.: *J. Master. Sci. Technol.* **28**(14), 313 (2012).
- [35] Y. Kumar et al., *Ceramics International* **42**, 5184 (2016).
- [36] Rabab khalid Sendi, Shahrom Mahmud, *Journal of Physical Science* **24**(1), 1 (2013).
- [37] G. Vijayaprashath et al., *Journal of Luminescence* **178**, 375 (2016).
- [38] N. F. Diaja et al., *Advances in Materials Physics and Chemistry, Science* **3**, 33 (2013).
- [39] J. Alejandro, J. M. Yanez-Limon, Jorge M. Seminario, *J. Phys. Chem. C* **115**, 282 (2011).

*Corresponding author: amirziaphysics@hotmail.com